ELECTRICAL PROPERTIES OF ANNEALED $La_{0.5}Sr_{0.5}MnO_3$ THIN FILMS PREPARED BY PULSED LASER DEPOSITION

E. Quenneville, P. Decorse, M. Meunier, F.Morin* and A.Yelon
Département de génie physique et de génie des matériaux
Ecole Polytechnique de Montréal
C.P. 6079, succ. Centre-ville
Montréal (Québec), Canada, H3C 3A7
* Institut de recherche d'Hydro-Québec (IREQ)
1800, boul. Lionel-Boulet,
Varennes (Québec), Canada, J3X 1S1

ABSTRACT

Conductivity measurements on $La_{0.5}Sr_{0.5}MnO_3$ thin films prepared by pulsed laser deposition are reported for different annealing conditions. In this paper, we use conductivity measurements to monitor film crystallization in real time during annealing. The annealing parameters used are: temperature ramps (1-5°C/min), oxygen partial pressures, p_{O2}, between 0.01 to 1.0 atm and $T_{plateau}$ (600-950°C). Under these conditions, the maximum conductivity obtained varied from 150 to 252 S/cm and the activation energy from 73.1 to 120 meV. The highest conductivity and the lowest activation energy have been obtained for 1°C/min in air and 1 hour plateau at 850°C. Under these conditions, the transition from an amorphous to a polycrystalline state lies between 590 and 601°C.

Key Words : Pulsed laser deposition, Thin films, lanthanum manganite, Conductivity measurements

INTRODUCTION

$La_{1-x}Sr_xMnO_3$, a perovskite ceramic, has received much attention as a candidate for the cathode material in solid oxide fuel cells (SOFCs). Particularly, $La_{0.5}Sr_{0.5}MnO_3$ (LSM5) fulfills all the principal requirements for this application: good catalytic activity for oxygen reduction, large electronic and ionic conductivity and compatibility with both the yttria-stabilized zirconia electrolyte and the interconnect material (1). There is still little work reported on electrical properties of LSM5 in bulk (2-5) or in thin film (6) forms.

In this study we show how the total conductivity of polycrystalline LSM5 thin films depends upon the annealing parameters. The objective is to find annealing parameters which will produce films with high conductivity and desirable structural properties. By measuring temperature and conductivity in-situ during annealing, the evolution of crystallization can be followed in real time. For example, it is possible to clearly identify the temperature at which the LSM5 film makes the transition from the amorphous to the perovskite structure.

In order to extract the maximum information from conductivity measurements, it is important to determine the main transport mechanism in LSM5. For similar compounds, it as been shown from various measurements (e.g. optical (7-9), thermoelectric power (10, 11), Hall effect (10)) that electronic conductivity is described by a polaronic mechanism. For example, while other models can describe σ vs. T at high temperature with good correlation, it can be shown, by measuring conductivity as a function of temperature from very low to high temperature, that the only mechanism which fits experimental data for this wide range is small polaron hopping (12-14).

Briefly, if the particle-lattice interaction is strong enough, delocalized electrons or holes can be trapped within potential wells created by the displacement of atoms from their carrier-free equilibrium position. Because it is the carrier itself which creates the well, this process is called "self-trapping" or "autolocalization". The quasi-particle formed by the carrier and the lattice distortion (phonons) is called a "polaron". If the carrier is localized more than 50% of the time on only one ion, the small polaron model is applicable. Electronic transport by small polarons will lead to an activated behavior at high temperature and to nearly metallic band conduction at low temperature. At high temperature, polaron conductivity, σ, is related to the hopping probability, P, by

$$\sigma = ne\mu = \frac{ne^2a^2}{k_BT}P \qquad [1]$$

where n, e, a, μ, T and k_B are respectively the polaron density, the electronic charge, the hopping distance, the polaron mobility, the temperature and the Boltzmann's constant. In this expression, P is given by (15)

$$P = p\nu_0 \exp\left(-\frac{W_H}{k_BT}\right) \qquad [2]$$

Here, ν_0 is the frequency of optical phonons, assuming no dispersion. This is the main frequency at which the carrier tries to hop to a neighboring site. W_H is the hopping energy (activation energy) and the Boltzmann factor $\exp(-W_H/k_BT)$ expresses the probability that two neighboring sites be in coincidence (in such a way that it is possible for the polaron to hop between the two sites).

The term, p, in Eq. [2] depends upon whether adiabatic (16) or non-adiabatic (17) the behavior is. This is important because it will lead to different interpretations of experimental results. In the adiabatic case, the carrier adjusts rapidly to the motion of the lattice, and on coincidence is very likely to hop to a neighboring site. Thus $p \cong 1$. Here, conductivity measurements fitted to a $\log(\sigma T)$ vs. $1/T$ plot should lead to a straight line. In the non-adiabatic case, the carrier moves too slowly in comparison with the lattice distortion and relaxation, and thus, it misses many coincidence events before making a hop. Then $p < 1$. It can be shown that in this case

$$p = \frac{2\pi}{h\upsilon_0}\left(\frac{\pi}{4W_Hk_BT}\right)^{1/2}J^2 \qquad [3]$$

In eq. [3], J, is half the electronic bandwidth for a rigid lattice, and h is Planck's constant. As opposed to the adiabatic model, data should be fitted to a $\log(\sigma T^{3/2})$ vs. 1/T plot to obtain straight lines. Thus, the activation energy obtained from the non-adiabatic model will be about 30% higher than the adiabatic value, and the data interpretation will be quite different. Even if both models fit our conductivity measurements quite well, it is possible to show that in LSM5 the appropriate polaronic motion is adiabatic (14).

EXPERIMENTAL

In the present work, pulsed laser deposition (PLD) was used to prepare LSM5 thin films. The experimental setup is described elsewhere (18). Films prepared under the conditions listed in Table I are amorphous.

Laser wavelength	248 nm
Repetition rate	30 Hz
Spot size	2 mm^2
Energy density	0.75 J/cm^2
Target-substrate distance	5.5 cm
Substrate	Sapphire (R-plane)
Substrate temperature	25°C
Deposition rate	≈ 100 Å/min

Table I. Pulsed laser deposition parameters

Targets for deposition were analyzed by x-ray photoelectron spectroscopy (XPS), energy dispersive x-ray spectrometry (EDX) and Rutherford backscattering spectrometry (RBS). These techniques showed that films have nominal LSM5 composition within experimental error for XPS and EDX (±2%). RBS also showed that the film composition is uniform throughout the bulk of the film. Film morphology was analyzed by scanning electron microscopy (SEM), by atomic force microscopy (AFM) and by x-ray diffraction (XRD). Amorphous films were dense and pinhole free. Depending upon the temperature plateau, annealed films can show some physical defects, caused principally by the film-substrate thermal expansion coefficient mismatch, which will be discussed later. XRD measurements confirmed that annealed films were polycrystalline and showed only the perovskite phase. Detailed results of these measurements are reported elsewhere (19).

The ionic contribution to the total conductivity of LSM5 is negligible in the bulk material due to the lack of departure from stoichiometry from any of the sublattices within the temperature and p_{O2} ranges under consideration (20). Thus the total conductivity is assumed to be purely electronic in what follows. Since electronic steady state is rapidly reached in thin films, it is possible to measure conductivity with a temperature ramp. Figure 1 shows a 4-point setup designed for high temperature total conductivity measurements of thin films. The main difficulties with such measurements are the establishment of good point contacts and the maintenance of their accurate positioning in

the presence of differential thermal expansion between materials. In order to avoid these problems, two platinum wire contacts were put on top of the sample and two beneath. The latter are put in contact with the film by use of platinum paste. To ensure good mechanical contact, the sample is held between an alumina capillary probe and a small alumina capillary placed on a pivot. If a small pressure is applied with the capillary probe on points over the film, because of the pivot, the small alumina capillary will rotate in order to ensure the good contact of the two point beneath the sample. This sits on an alumina tube which also acts as a gas inlet. This system is placed inside a quartz tube heated by a furnace.

Four samples, prepared under the conditions of Table I, were treated under two different pressures of O_2 (different fractions O_2/N_2 of total pressure of 1 bar), subjected to two different rates of temperature increase to either final plateau temperatures 850 or 950°C, and held at plateau for varying times. These are given in Table II. After cooling and measurement the sample annealed at 850°C were brought back to that temperature, or to somewhat higher temperature, as shown in the table.

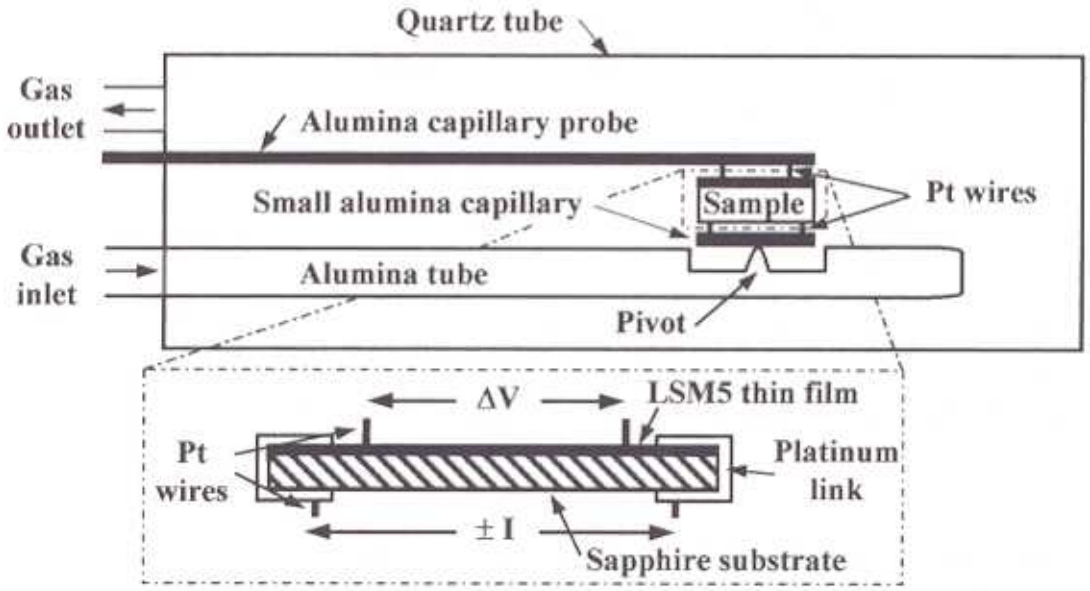

Figure 1. 4-point experimental setup for high temperature measurements

RESULTS

Since samples prepared under the conditions given in Table I are amorphous, they must be annealed to obtain dense crystalline films. Since amorphous LSM5 is an insulator and crystalline LSM5 is a good electrical conductor, conductivity measurements during annealing can be used to monitor the crystallization of the film. Figure 2a shows $\log(\sigma T)$ as a function of 1000/T during the annealing of an amorphous thin film of LSM5. As we can see from this graph, the resistance of the film is too high to be measurable by our system below 338°C ($R>120\ M\Omega$). When conductivity becomes measurable, it increases slowly up to 590°C. We attribute the abrupt increase in conductivity at this

temperature to the phase transition from the amorphous to the perovskite structure. This transition was confirmed by x-ray diffraction analysis. XRD and AFM measurements performed on films annealed at different temperatures between 600 and 850°C showed an enhancement in the film's crystallization with increased annealing temperature. Peaks in the XRD spectra are sharp, narrowing with increasing temperature. AFM imaging shows that the grain size went from about 80 nm at 600°C to 240 nm at 850°C. Figure 2b shows an enlargement of the region where the temperature is held at the plateau for 1 hour. A certain temperature overshoot (less than 5°C) is observed, but temperature stabilize at $T_{plateau}$ in less than five minutes. During the plateau, the conductivity is increased by $\Delta\sigma_{plateau}$. The conductivity enhancement is important at the beginning and becomes negligible after 1 hour.

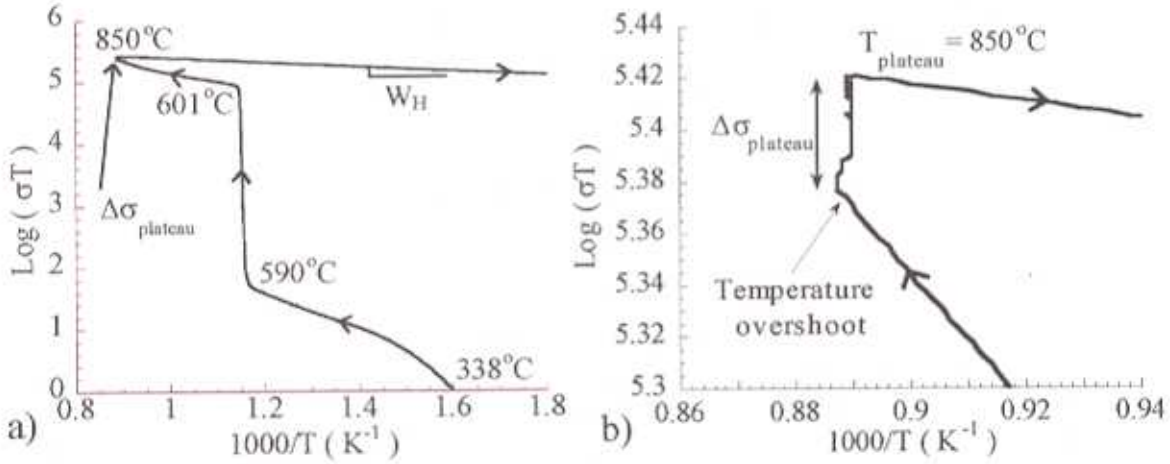

Figure 2a. Log(σT) as a function of 1000/T for sample 3 (run 3-1) when annealed from RT to $T_{plateau}$ = 850°C. After annealing, the sample was slowly cooled down to RT at 5°C/min. Figure 2b is an enlargement of the temperature plateau region of Figure 2a.

After the temperature plateau, conductivity measurements were made as the sample slowly cooled down to room temperature (5°C/min) as seen in Figure 2a. The conductivity was measured again as the temperature was raised from RT to $T_{plateau}$ (5°C/min). For all runs, both curves are superimposed, even at the highest temperatures, indicating that no further structural change took place.

For thin films prepared under the same deposition conditions (Table I), the conductivity behavior after annealing changes with the annealing conditions. As mentioned earlier, if the adiabatic small polaron model can describe the behavior of the carriers in annealed LSM5 thin films, the plot of log(σT) vs. 1/T should be linear. This is indeed the case for each run (Figure 3). However, for runs 1-1, 4-1, 4-2 and 4-3 it is possible to observe small deviations from linearity at high temperatures.

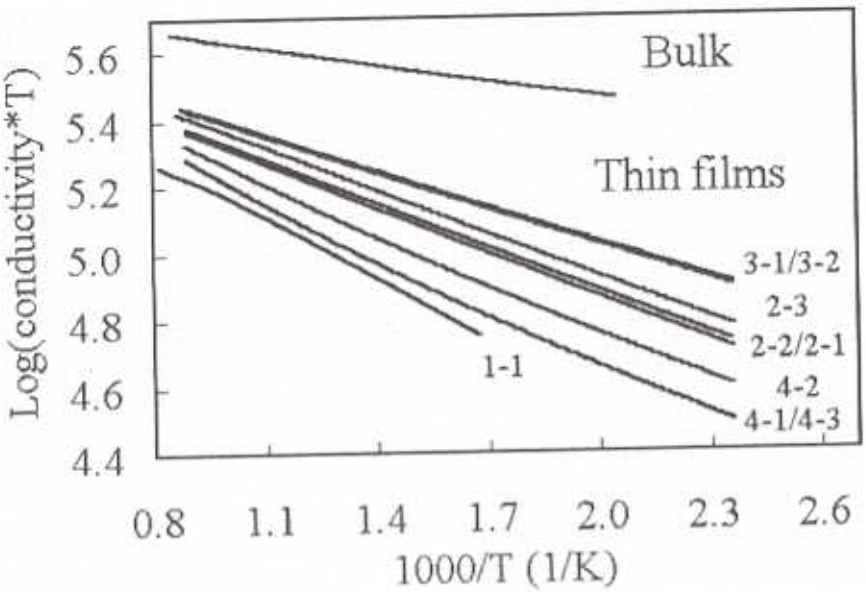

Figure 3. Comparison between conductivity measurements done on bulk and on thin films annealed under different conditions, which are given in Table II.

Table II summarizes the annealing parameters for the four samples, as well as measured parameters related to crystalline and electrical properties of the LSM5 films. $T_{transition}$ represents the temperature range where there is an abrupt increase in conductivity attributed to the transition from the amorphous to the perovskite structure. The maximal conductivity recorded during cooling, σ_{max}, is also shown. Conductivity was also recorded during the temperature plateau and $\Delta\sigma_{plateau}$ is the conductivity difference between the end and the beginning of the plateau. Subsequent thermal treatments have been done at higher temperatures for three samples after the first annealing. Measured parameters are also presented in those cases. The activation energy (hopping energy), W_H, and the linear correlation coefficient, R^2, (obtained with the cooling data and expressed according to the adiabatic polaron model) are also presented. The reason why $T_{transition}$ is higher for sample 1 than for any other samples is that all the other samples have been preheated for 30 minutes at 250°C in order to evaporate all solvents in the platinum paste before annealing.

Runs	Imposed parameters				Measured parameters				
	p_{O2} (%)	dT/dt_{init} (°C/min)	$T_{plateau}$ (°C)	$t_{plateau}$ (h)	$T_{transition}$ (°C)	σ_{max} (S/cm)	$\Delta\sigma_{plateau}$ (S/cm)	R^2	W_H (meV)
1-1	21	5	950	0.5	693-725	149.6	-28	0.9987	120
2-1	21	5	850	0.5	601-625	207.5	+38	0.9999	90.9
2-2	21	-	850	12	-	226.9	+10	0.9999	81.6
3-1	21	1	850	1	590-601	248.0	+22	0.9999	74.1
3-2	21	-	865	12	-	251.9	0	0.9999	73.1
3-3	21	-	885	12	-	231.3	-12	0.9999	87.3
4-1	100	1	850	12	612-631	168.1	+25	0.9989	115
4-2	21	-	850	12	-	188.6	+18	0.9995	106

4-3	100	-	850	12	-	170.0	-17	0.9989	118

Table II. Annealing parameters for the four different samples

In order to observe the oxygen partial pressure dependence of the conductivity for annealed LSM5 films, conductivity vs. temperature was measured under different oxygen environment. Figure 4 shows log(σT) as a function of 1000/T for sample 3 after its first annealing at 850°C for three runs in different oxygen partial pressures (0.01, 0.21 and 1.0 atm). The three straight lines obtained were identical, so the conductivity is clearly not a function of oxygen partial pressure between 0.01 and 1.0 atm.

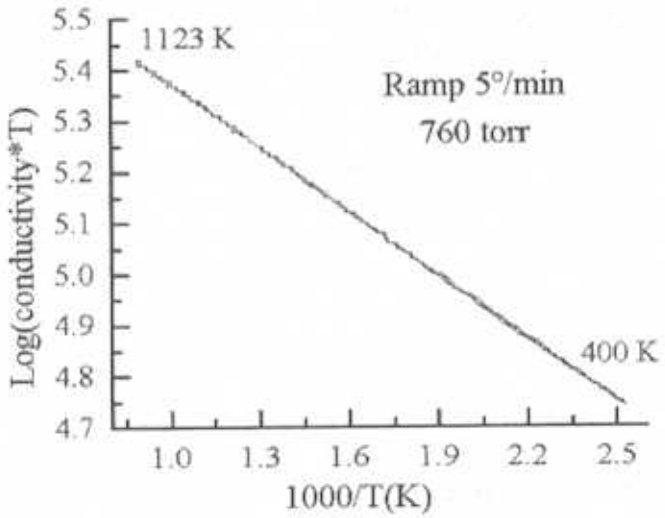

Figure 4. Log(σT) vs. 1000/T for LSM5 at P_{O2} = 0.01, 0.21 and 1.0 atm.

DISCUSSION

The activation energy and the linear correlation coefficient can be used to quantify the properties of the film. It was proposed (13, 21) that the hopping energy is in direct relationship with the Mn-O-Mn bond angle in the perovskite structure. Minimum hopping energy is obtained for a totally relaxed structure. Because of the LSM5/sapphire thermal expansion coefficient mismatch (TEC_{LSM5}= 13.5 x 10^{-6} and $TEC_{Sapphire}$ = 7.7 x 10^{-6}), elastic energy is accumulated into the film as samples are heated. Above 700°C, newly annealed films may dissipate some of this energy by inducing physical defects. Defects such as partial delamination, cracks and film lift up could be observed by SEM and by optical microscopy on a certain number of samples, but appeared only to a limited extent. Moreover, these defects did not develop further upon heating again the same films up to the same temperature limits. The main effect expected from such defects would be an apparent reduction of the film conductivity. Being mostly geometrical in nature, this effect would normally not affect conductivity slopes. There is however a critical temperature above which physical damages start to occur repeatedly. By looking at the successive annealings done on sample 3 and by comparing runs 1-1 and 2-1 it is possible

to determine that this critical temperature is very close to 865°C. For this reason, a relationship between hopping energy and $T_{plateau}$ is evaluated only for temperatures below this critical temperature. Due to its superior insulating behavior, sapphire has been preferred here to other single crystal substrates with lower mismatch coefficients like $LaTiO_3$ or yttrium-stabilized zirconia. A good alternative substrate could be provided by $LaAlO_3$ single crystals. Nonetheless, it remains to be confirmed that the degradation is not also related with additional phenomena like facetting or chemical degradation at the LSM5/substrate interface above the critical temperature.

On the assumption that the adiabatic polaron model can be applied to recrystallized film, the hopping energy should be constant during cooling. The linear correlation coefficient, R^2, which shows the agreement of the data with the adiabatic small polaron model, can thus be used to determine if the hopping energy varies or not within any single run. The closer this coefficient is to 1, the more constant is the hopping energy. Table II shows such an agreement with R^2 almost equal to one for all runs with samples 2 and 3. For the remaining samples, 1 and 4, R^2 slightly decreases. Lower conductivities are also observed for these samples. Run 1-1 was performed up to a significantly higher temperature, e.g. 950°C. It may well be that this sample was irreversibly modified. Sample 4 was a distinct case since the first recrystallization annealing was performed in pure oxygen and two different atmospheres were used during successive runs. There is a clearly reversible effect of the surrounding atmosphere upon the conductivity curves, the hopping energy being raised and the conductivity lowered by annealing in pure oxygen. It remains to be confirmed whether this phenomenon is governed or not by a diffusion process in the high temperature region of the corresponding runs.

The time during which the temperature is held at the plateau, $t_{plateau}$, will also have an important effect on the crystallization of the film. The optimum duration of the plateau depends upon the annealing parameters and especially on $T_{plateau}$. For a given $T_{plateau}$, different behavior can be observed when film conductivity is monitored. When it is under 865°C, the film conductivity is enhanced with increasing $t_{plateau}$. The time needed to obtained constant maximum conductivity is about one hour and is nearly the same for different $T_{plateau}$ ranging from 700 to 850°C. For $T_{plateau}$ over the critical temperature, the conductivity decreased sharply with $t_{plateau}$. For example, with sample of run 1-1, annealed at 950°C, the conductivity reduction for only 30 minutes is $\Delta\sigma_{plateau}$ = -28 S/cm. At the critical temperature (~865°C), an intermediate case is observed. With a 12 hour plateau, the conductivity increased by 4 S/cm for the first 4 hours, and then, decreased by 4 S/cm during the rest of the plateau, resulting in no net variation of film conductivity.

CONCLUSION

There are at least four parameters which should be controlled in order to anneal amorphous LSM5 thin films. (i) A slow initial temperature ramp leads to higher conductivity values. A 1°C/min ramp is a good compromise between such a result and the time needed to reach $T_{plateau}$. (ii) Since amorphous LSM5 shows a small oxygen deficiency, a partial oxygen pressure, p_{O2}, is needed during annealing. Runs performed in air lead to higher conductivity than in pure oxygen at atmospheric pressure. (iii) The temperature at which the temperature is held constant has a significant effect on

stabilizing film electrical properties. It should be as high as possible and remain compatible with reproducible results between successive runs. On the basis of our results, this temperature is slightly below 865°C. (iv) The time during which $T_{plateau}$ is maintained is another important parameter. After one hour at 850°C, we observed that the conductivity enhancement is near maximum. Electrical conductivity of annealed LSM5 thin films is lower than bulk values. Films deposited on substrate presenting a lower thermal expansion coefficient mismatch with LSM5 than sapphire remain to be investigated.

ACKNOWLEDGMENTS

The authors thank the Natural Sciences and Engineering Research Council of Canada (NSERC) and Hydro-Quebec Research Institute (IREQ) for financial support. They also acknowledge Dr. Abdeltif Essalik and Dr. Lyne M. Cormier for useful discussions, and Jean-Paul Lévesque for technical support.

REFERENCES

1. V.E.J. Van Dieten, J.P. Dekker and J. Schoonman, Mat. Res. Soc. Symp. Proc., **369**, 669 (1995)
2. A. Hammouche, E.J.L. Schouler and M. Henault, Solid State Ionics, **28-30**, 1205-1207 (1988)
3. K. Katayama, T. Ishihara, H. Ohta, S. Takenchi, Y. Esaki and E. Inukai, Nippon Seramikkusu Kyokai Gakujutsu Ronbunshi, **97**, 1327-33 (1989)
4. H. Lauret, E. Caignol and A. Hammou, Proceeding of the Second International Symposium on Solid Oxide Fuel Cells, P.Zeghers, 479-486 (1991)
5. J.A.M. van Roosmalen, J.P.P. Huijsmans and L. Plomb, Solid State Ionics, **66**, 279-284 (1993)
6. B. Gharbage, F. Mandier, H. Lauret, C. Roux and T. Pagnier, Solid State Ionics, **82**, 85-94 (1995)
7. A. Machida, Y. Moritomo, and A. Nakamura, Physical Review B, **58**, 8, R4281 (1998)
8. S. Yoon, H.L. Liu, G. Schollerer, S.L. Cooper, P.D. Han, D.A. Payne, S.-W. Cheong, and Z. Fisk, Physical Review B, **58**, 5, 2795 (1998)
9. Y.G. Zhao, J.J. Li, R. Shreekala, H.D. Drew, C.L. Chen, W.L. Cao, C.H. Lee, M. Rajeswari, S.B. Ogale, R. Ramesh, G. Baskaran, and T. Venkatesan, Physical Review Letters, **81**, 6, 1310 (1998)
10. M. Jaime, M.B. Salomon, M. Rubinstein, R.E. Treece, J.S. Horwitz, and D.B. Chrisey, Physical Review B, **54**, 17, 11914 (1996)
11. M.F. Hundler and J.J. Neumeier, Physical Review B, **55**, 17, 11511 (1997)
12. D.C. Worledge, G. Jeffrey Snyder, M.R. Beasley, T.H. Geballe, R. Hiskes, and S. DiCarolis, J. Appl. Phys., **80**, 9, 5158 (1996)
13. M. Jaime, H.T. Hardner, M.B. Salomon, M. Rubinstein, P. Dorsey, and D. Emin, Phys. Rev. Lett., **78**, 5, 951 (1997)
14. E. Quenneville, M. Meunier, A. Yelon and F. Morin, to be published

15. W.E. Spear, Advances in Physics, **23**, 3, 523 (1974)
16. D. Emin and T. Holtein, Annals of Physics, **53**, 439-520 (1969)
17. T. Holtein, Annals of Physics, **8**, 343-389 (1959)
18. R. Izquierdo, F. Hanus, Th. Lang, D. Ivanov, M. Meunier, L. Laude, J.F. Currie and A.Yelon, Appl. Surf. Sci., **96-98**, 855 (1996)
19. P. Decorse, E. Quenneville, M. Meunier, A.Yelon and F. Morin, to be published
20. H. Tagawa, N. Mori, H. Takai, Y. Yonemura, H. Minaniue, H. Inaba, J. Mizusaki, and T. Hashimoto, Proc. of the 5th International Symposium on Solid Oxide Fuel Cells, **PV97-40**, 795-804 (1997)
21. J.M. De Teresa, K. Dörr, K.H. Müller, and L. Schultz, Physical Review B, **58**, 10, R5928 (1998)